

Sound Radiation from a Concave or a Convex Dome in a Semi-Infinite Tube*

HIDEO SUZUKI**

CBS Technology Center, Stamford, CT 06905, USA

The radiation characteristics of concave and convex domes in a semi-infinite lossless tube are discussed. If the diaphragm is not flat, the far-field sound pressure (normalized to the pressure of the flat piston) is not constant. A peak of 0.5–0.7 dB is observed around the normalized frequency range of $kA = 2.2$ – 2.8 (where A is the radius of the tube). The response then falls abruptly as the frequency approaches the value of the first radial mode ($kA = 3.83$). The radiation resistance is proportional to the sound pressure since any loss in the tube is ignored. The imaginary part of the radiation impedance shows large negative values in the high-frequency range ($kA \geq 2.5$).

0 INTRODUCTION

One-dimensional wave propagation is a simple mathematical problem, and this type of propagation is also easily achieved by the use of a long wave tube. For this reason, the air column has been used for different kinds of studies of acoustics. The application of one-dimensional wave propagation in a wave tube has been used to study four areas:

- 1) Classical investigation of the acoustical properties of a gas. Kundt measured the sound velocities in tubes with different diameters and gases [1], [2].
- 2) Measurement of the absorption coefficient (acoustical impedance) of materials [3], [4]. The "impedance tube" has played a significant role in room acoustics and noise control.
- 3) Measurement of amplitude frequency responses of high-frequency drivers [5]. The wave tube simplifies the boundary conditions of the radiation from the driver and is also expected to give a constant radiation impedance.
- 4) Study of the nonlinear acoustical properties of a gas. Since the pressure decrease of sound with increasing distance is minimal for one-dimensional wave propagation, nonlinear effects are more easily observed in the tube.

Except for the third application, more interest is

placed on the sound propagation of the far field from the source than of the near field. In these cases, the assumption of one-dimensional wave propagation is well met since only a plane wave can travel a long distance inside the tube.

In the third application, however, the near field as well as the far field is important since the radiation characteristics are effected significantly by the boundaries near the driver. Mostly the driver has a nonflat diaphragm that produces a two- or three-dimensional sound field. Therefore it is important to investigate the effect of the diaphragm shape on the accuracy of this measurement. Recently the effects of the diaphragm shapes of convex and concave radiators in an infinite baffle were investigated [6]–[9], and it was found that a concave or a convex radiator in an infinite baffle has different radiation characteristics than a flat diaphragm with the same radius. A similar result is expected for the nonflat diaphragm in a semi-infinite tube. The radiation resistance may deviate from the expected value, and if this is the case, the radiation reactance may have nonzero values in the same frequency range. In this paper the pressure responses and the radiation impedance responses of convex and concave domes in a semi-infinite tube are discussed. The frequency range of interest is limited below the frequency corresponding to the first radial mode, which covers the typical reproduction range of the driver.

* Manuscript received 1983 November 15; revised 1985 August 1.

** Present Address: Ono Sokki Company Ltd., Shinjuku, Tokyo 160, Japan.

1 LIST OF SYMBOLS

| | |
|------------------------------|--|
| A | radius of dome |
| B_{mn} | matrix converting $\{a_n\}$ to $\{b_m\}$ |
| E | square error |
| EI | error index |
| H | height of dome |
| I | intensity |
| $J_n(\cdot)$ | n th-order cylindrical Bessel function |
| M, N | maximum values of orders m and n , respectively |
| O, O' | origins of coordinate systems |
| $P_n(\cdot)$ | n th-order Légendre functions of the first kind |
| S_1 | radiator surface |
| S_2 | imaginary surface of dome opening |
| S_3 | surface of short tube |
| U_0 | velocity amplitude of dome in z direction |
| W | radiated power |
| Z | radiation impedance |
| Z_R | radiation resistance |
| a_n, b_m | unknown coefficients |
| c | velocity of sound |
| i | imaginary unit, $= \sqrt{-1}$ |
| $j_n(\cdot)$ | n th-order spherical Bessel function |
| k | wavenumber |
| k_m | number satisfying $J_1(k_m) = 0$ |
| l, m, n | orders of functions |
| r | radius of cylindrical coordinate system |
| r_1 | radius of polar coordinate system |
| $u_\nu(\cdot)$ | velocity component of ν direction |
| z | axial component of cylindrical coordinate system |
| $\Psi_n^{(1)}, \Psi_n^{(2)}$ | functions defined on surfaces S_1 - S_3 |
| θ | cone angle of spherical coordinate system |
| θ_ν | angle of unit vector measured with respect to z axis |
| κ_m | number given by $\kappa_m^2 = k^2 - k_m^2$ |
| ν | unit vector normal to surfaces S_1 - S_3 |
| ρ | density of air |
| ψ_I, ψ_{II} | velocity potentials |
| ω | angular frequency |
| $*$ | complex conjugate |

2 GEOMETRY OF THE SYSTEM

The present method, which was used in [7]-[10], can be applied to an arbitrarily shaped radiator. In the present case, however, this method is more suitable for the radiation from a concave dome than from a convex dome. This leads us to use two different geometries for the concave and convex domes.

Fig. 1(a) shows the geometry of the system with a concave dome. The origin O is taken at the center of the end of the semi-infinite tube (opening of the dome). The cylindrical coordinate system (r, z) is used inside the tube, and the spherical coordinate system (r_1, θ) is used inside the dome. The surfaces of the dome and

the end of the semi-infinite tube are denoted by S_1 and S_2 , respectively.

Fig. 1(b) shows the geometry of the system with a convex dome. The origin O of the cylindrical coordinate system (r, z) is at the top of the dome. The origin O' of the spherical coordinate system (r_1, θ) can be arbitrary, even though the accuracy is highly dependent on the location of this origin. The notations S_1 and S_2 are the same as in Fig. 1(a). The surface of the short tube connecting S_1 and S_2 is denoted by S_3 . In both cases the radiator vibrates as a piston with velocity U_0 in the z direction, and with angular frequency ω .

3 MATHEMATICAL DISCUSSION

The method used here is called the least-square error method, and the application of this method to a general radiation problem is given in [10]. The mathematical discussion here will be limited to the radiation problem from the convex dome only, since it is more complex than the problem of the concave dome.

The velocity potential inside the space surrounded by S_1, S_2 , and S_3 is represented by

$$\psi_I(r_1, \theta) = \sum_{n=0}^{\infty} a_n j_n(kr_1) P_n(\cos \theta) \tag{1}$$

The velocity potential of the wave propagating to the positive z direction in the tube is represented by

$$\psi_{II}(r, z) = \sum_{m=0}^{\infty} b_m e^{-i\kappa_m z} J_0\left(\frac{k_m}{A} r\right) \tag{2}$$

where $J_0(k_m r/A)$ satisfies the orthogonal condition

$$\int_0^A r J_0\left(\frac{k_m}{A} r\right) J_0\left(\frac{k_n}{A} r\right) dr = \frac{A^2}{2} J_0^2(k_m), \quad m = n$$

$$= 0, \quad m \neq n \tag{3}$$

The particle velocity on S_1 and S_3 in the direction of ν is obtained by

$$u_\nu(r_1, \theta) = -\left(\frac{\partial \psi_I}{\partial r_1} \frac{\partial r_1}{\partial \nu} + \frac{\partial \psi_I}{\partial \theta} \frac{\partial \theta}{\partial \nu}\right)$$

$$= \sum_{n=0}^{\infty} a_n \Psi_n^{(1)}(r_1, \theta) \tag{4}$$

where

$$\Psi_n^{(1)}(r_1, \theta) = -[kj_n'(kr_1)P_n(\cos \theta)\cos(\theta_\nu - \theta)$$

$$- j_n(kr_1)P_n'(\cos \theta) \sin \theta \sin(\theta_\nu - \theta)/r_1] \tag{5}$$

This must be equal to the prescribed velocity distributions on surfaces S_1 and S_3 . Thus we have

$$\sum_{n=0}^{\infty} a_n \Psi_n^{(1)}(r_1, \theta) = U_0 \cos \theta_\nu, \quad \text{on } S_1$$

$$= 0, \quad \text{on } S_3. \quad (6)$$

On surface S_2 the velocity potential and the particle velocity normal to the surface must be continuous, that is,

$$\psi_I(r_1, \theta) = \psi_{II}(r, z), \quad \text{on } S_2 \quad (7)$$

and

$$-\frac{\partial \psi_I(r_1, \theta)}{\partial \nu} = -\frac{\partial \psi_{II}(r, z)}{\partial z}, \quad \text{on } S_2 \quad (8)$$

where the unit vector ν is parallel to the z axis on surface S_2 ($z = 0$). From Eq. (7) using the orthogonality condition Eq. (3), we have

$$b_m = \sum_{n=0}^{\infty} a_n B_{mn} \quad (9)$$

where

$$B_{mn} = \frac{2}{A^2 J_0^2(k_m)} \int_0^A r J_0\left(\frac{k_m}{A} r\right) j_n(kr_1) P_n(\cos \theta) dr. \quad (10)$$

Eq. (8) can be rewritten as

$$-\sum_{n=0}^{\infty} a_n [kj'_n(kr_1) P(\cos \theta) \cos(\theta_\nu - \theta) - j_n(kr_1) P'(\cos \theta) \sin \theta \sin(\theta_\nu - \theta)/r_1]$$

$$= -\sum_{m=0}^{\infty} b_m (-i\kappa_m) J_0\left(\frac{k_m}{A} r\right). \quad (11)$$

Substituting Eq. (9) into Eq. (11), we have

$$\sum_{n=0}^{\infty} a_n \Psi_n^{(2)} = 0, \quad \text{on } S_2 \quad (12)$$

where

$$\Psi_n^{(2)}(r_1, \theta) = [kj'_n(kr_1) P_n(\cos \theta) \cos(\theta_\nu - \theta) - j_n(kr_1) P'_n(\cos \theta) \sin \theta \sin(\theta_\nu - \theta)/r_1]$$

$$+ \sum_{m=0}^{\infty} i\kappa_m J_0\left(\frac{k_m}{A} r\right) B_{mn}. \quad (13)$$

Now if we truncate the orders m and n by M and N , respectively, Eqs. (6) and (12) are not exactly satisfied, and the square error can be defined as

$$E = \int_{S_1} \left| \sum_{n=0}^N a_n \Psi_n^{(1)}(r_1, \theta) - U_0 \cos \theta_\nu \right|^2 dS$$

$$+ \int_{S_3} \left| \sum_{n=0}^N a_n \Psi_n^{(1)}(r_1, \theta) \right|^2 dS$$

$$+ \int_{S_2} \left| \sum_{n=0}^N a_n \Psi_n^{(2)}(r_1, \theta) \right|^2 dS. \quad (14)$$

The least-square error method allows us to minimize Eq. (14). This is done by differentiating Eq. (14) with respect to a_n , $n = 0, 1, \dots, N$, so that we obtain $N + 1$ simultaneous equations:

$$\sum_{n=0}^N a_n [\int_{S_1+S_3} \Psi_n^{(1)} \Psi_l^{(1)*} dS + \int_{S_2} \Psi_n^{(2)} \Psi_l^{(2)*} dS]$$

$$= \int_{S_1} U_0 \cos \theta_\nu \Psi_l^{(1)*} dS, \quad l = 0, 1, 2, \dots, N. \quad (15)$$

The solution of Eq. (15) gives the optimum set of coefficients $\{a_n\}$ in the sense that the square error defined by Eq. (14) is minimum. Once $\{a_n\}$ is determined, $\{b_m\}$ is given by Eq. (9).

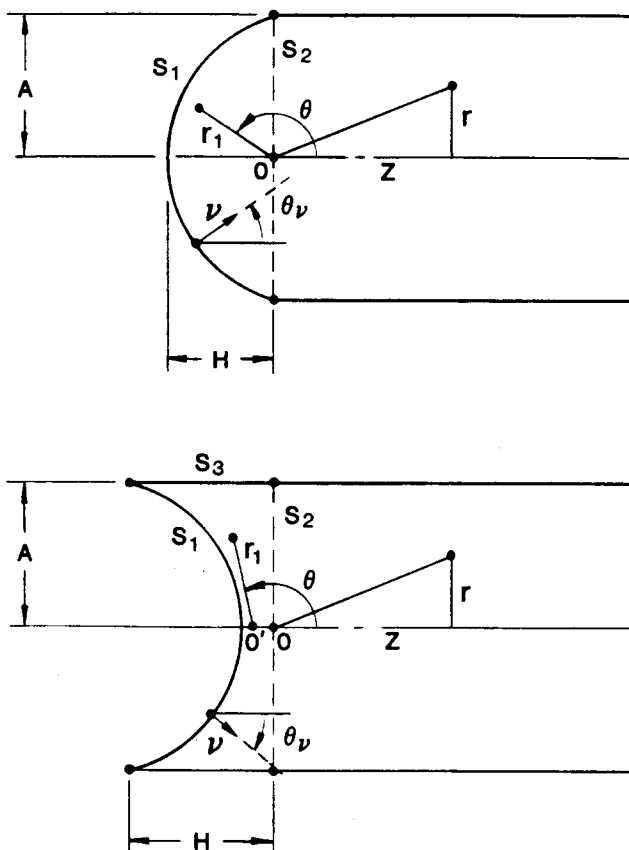


Fig. 1. Geometry of system with (a) a concave dome or (b) a convex dome radiator in a semi-infinite tube.

4 RESULTS AND DISCUSSION

The computer used for the present study was a mini-computer (PDP 11/70). The values of the height-to-radius ratio H/A used for the calculation were 0.5, 0.7, and 1.0 for the concave dome, and 0.5 and 0.7 for the convex dome. The accuracy of the results depends significantly on the orders of the truncation M and N . M and N (which were chosen such that $M = N$ in the present study) were 7 for the concave dome, and 12 ($H/A = 0.5$) and 14 ($H/A = 0.7$) for the convex dome. The reason why larger numbers of M and N are needed for the convex dome than for the concave dome is that $\Psi_1(r_1, \theta)$ must satisfy a more complex boundary condition in the problem of the convex dome. The accuracy of the result is discussed in more detail in Section 4.3.

4.1 Sound Pressure Response

Below the frequency corresponding to the first radial mode, only the pistonlike plan wave can propagate. Then the far-field sound pressure in the tube normalized to the sound pressure of a flat piston is given by

$$\left| \frac{\psi_1(\text{fairfield})}{\psi(\text{piston})} \right| = \frac{\omega \rho b_0}{\rho c U_0} = \frac{k b_0}{U_0} \quad (16)$$

The results of the concave dome are shown in Figs. 2-4 for $H/A = 0.5, 0.7,$ and $1.0,$ respectively. The pressure response rises gradually and then drops off very quickly as the frequency approaches the cut-off frequency ($kA = 3.83$). The peak values are 0.52 dB at $kA = 2.8, 0.66$ dB at $kA = 2.5,$ and 0.69 dB at $kA = 2.2$ for $H/A = 0.5, 0.7,$ and $1.0,$ respectively. A direct radiator type driver with $A = 1$ cm may be used in the frequency range of 5 kHz ($kA = 0.94$) to 20 kHz ($kA = 3.8$). Thus for the measurement of the driver response, the frequency range of $kA = 2-3$ is very important. The increase of the radiation efficiency by 0.5-0.7 dB in this range may not be significant in

so far as the contributions of other error factors in the measurement of the frequency response will dominate. The frequencies at which the response shows a 1-dB decrease are $kA = 3.6, 3.4,$ and 3.1 for $H/A = 0.5, 0.7,$ and $1.0,$ respectively. These frequencies may be considered the limiting frequencies for the measurement of the sound pressure response. It should be noted, however, that this is valid only when the diaphragm vibrates as a piston.

The pressure responses of the convex dome are shown in Figs. 5 and 6 for $H/A = 0.5$ and $0.7,$ respectively. The response for $H/A = 1.0$ is not shown because the expected accuracy was not achieved in this case. The responses of the convex dome are very similar to those of the concave dome. This indicates that convex and concave radiators with approximately the same heights or depth-to-radius ratios will behave quite similarly.

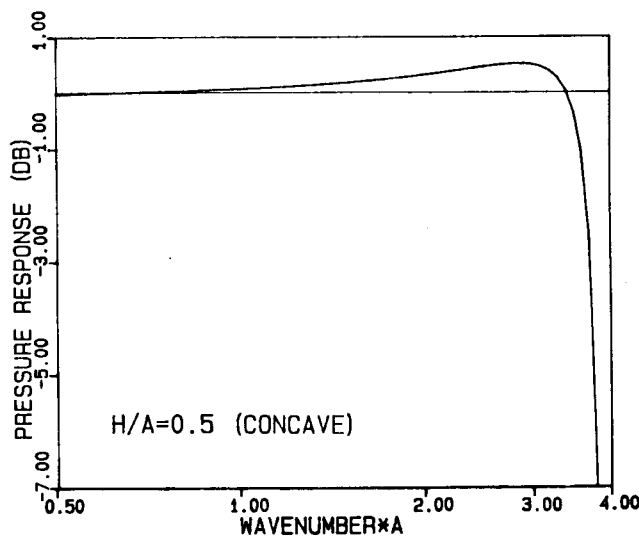


Fig. 2. Normalized sound pressure response of a concave dome with $H/A = 0.5$ in a semi-infinite tube.

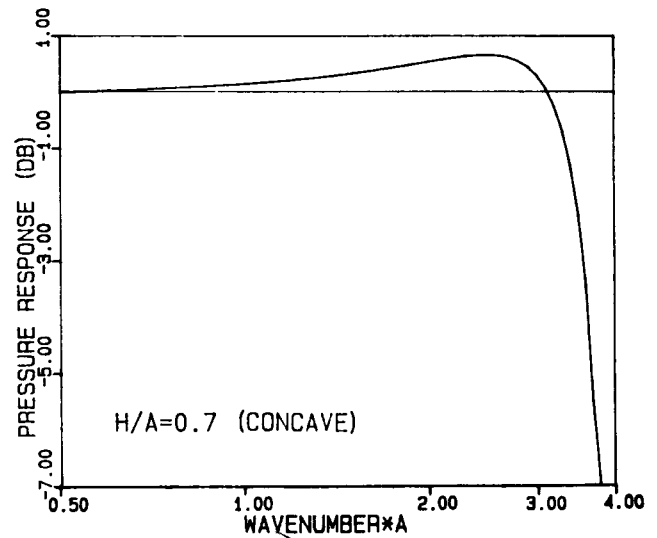


Fig. 3. Normalized sound pressure response of a concave dome with $H/A = 0.7$ in a semi-infinite tube.

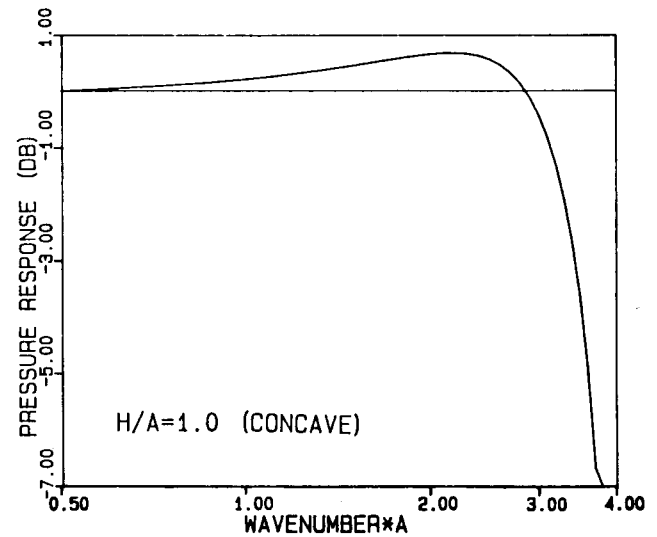


Fig. 4. Normalized sound pressure response of a concave dome with $H/A = 1.0$ in a semi-infinite tube.

4.2 Radiation Impedance

The time-averaged intensity on the surface of the diaphragm is calculated by

$$I = i\omega\rho\psi_1(r_1, \theta)U_0 \cos \theta_v/2 . \tag{17}$$

The total radiated power is then obtained by

$$W = \int_{S_1} I \, dS . \tag{18}$$

The normalized radiation impedance is calculated by dividing Eq. (18) by the power radiated by the flat piston such as

$$Z = 2W/\rho c\pi A^2 U_0^2 . \tag{19}$$

The result is shown in Figs. 7-9 for the concave dome and in Figs. 10 and 11 for the convex dome. The upper

curve shows the radiation resistance and the lower curve the radiation reactance. If there is no error in the calculation, the normalized sound pressure response is calculated from the radiation resistance by $10 \log Z_R$. The differences between the peak values of the pressure response given in Section 4.1 and the peak values calculated from the radiation resistance are less than 0.02 dB for the concave dome and less than 0.04 dB for the convex dome. These values are a good indication of the accuracy of the results. It is worthwhile to find out the ratio of the radiation resistance to the sum of the electromagnetic and mechanical dampings of a driver. For example, a dome loudspeaker with $A = 1 \text{ cm}$, $Q_0 = 1$, $M_0 = 0.2 \text{ gram}$, and $f_0 = 1 \text{ kHz}$ has a damping of $1.26 \, \Omega$ (MKS). The radiation resistance is approximately 10% of the sum of the electromagnetic and mechanical dampings. From this example it is expected that the contribution of the radiation resistance to the

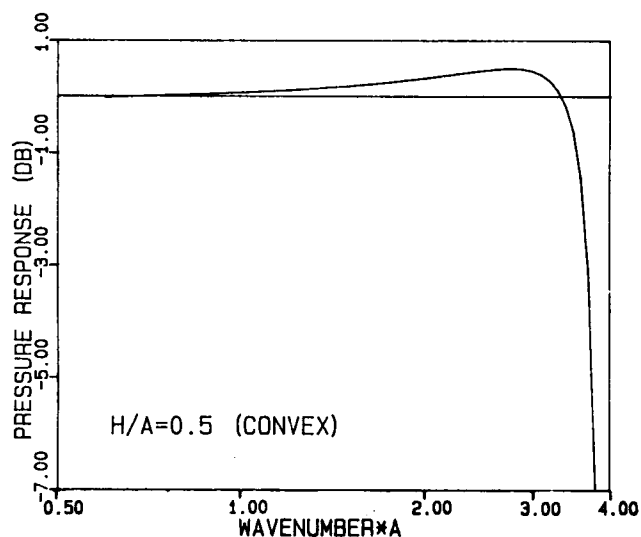


Fig. 5. Normalized sound pressure response of a convex dome with $H/A = 0.5$ in a semi-infinite tube.

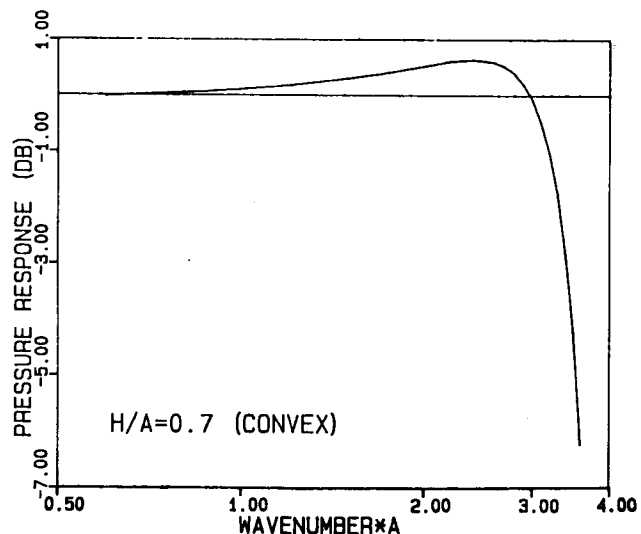


Fig. 6. Normalized sound pressure response of a convex dome with $H/A = 0.7$ in a semi-infinite tube.

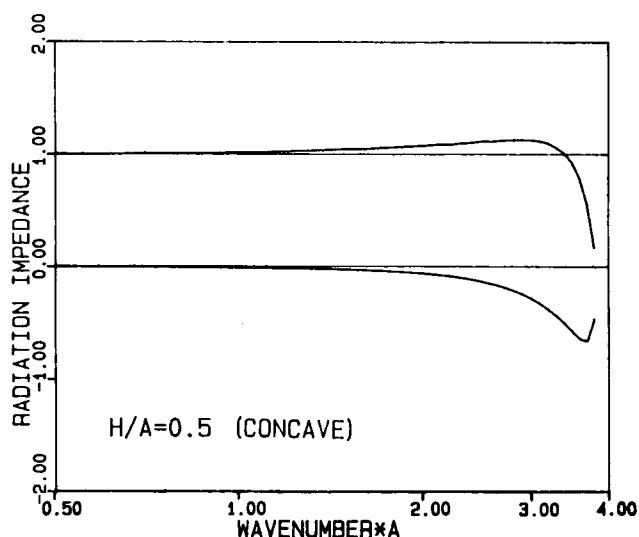


Fig. 7. Normalized radiation resistance (upper curve) and radiation reactance (lower curve) of a concave dome with $H/A = 0.5$ in a semi-infinite tube.

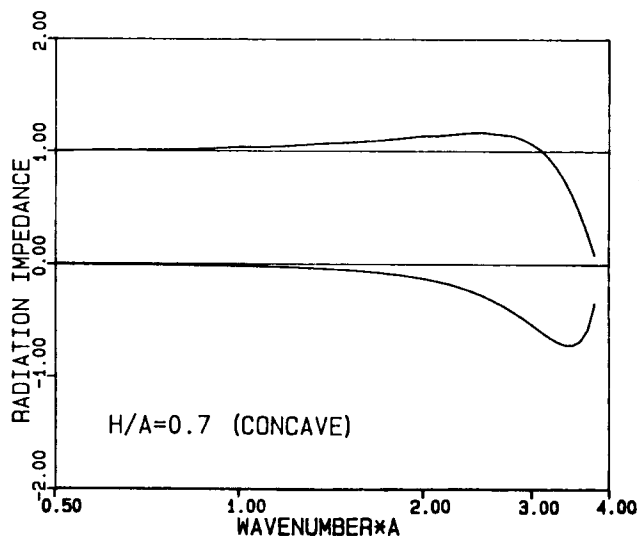


Fig. 8. Normalized radiation resistance (upper curve) and radiation reactance (lower curve) of a concave dome with $H/A = 0.7$ in a semi-infinite tube.

total damping may not exceed 20% for most cases.

The radiation reactance curve starts from zero and gradually becomes negative, showing the minimum below the cut-off frequency. A big difference between the radiation reactances of the radiators in the infinite baffle and in the semi-infinite tube is that the latter always stays springlike (i.e., the imaginary part of the impedance is negative) below the first resonance frequency. The effect of the radiation reactance on the motion of a loudspeaker diaphragm appears to be negligible, since it is much smaller than the reactance due to the mass of the diaphragm in most practical cases.

4.3 Accuracy of Results

Since the true values are unknown, it is necessary to have some indexes to evaluate the accuracy of the results. The matching of the normalized sound pressure shown in Section 4.1 and the response obtained by $10 \log Z_R$ from Section 4.2 is one of those indexes. As was discussed in Section 4.2, the differences were less than 0.02 dB for the concave dome and less than 0.04 dB for the convex dome, both at peak frequencies. It is expected that the magnitude of error (dB deviation from the unknown true value) may be in the same order with these differences.

Another way of estimating the accuracy is to check the degree of matching of the velocity potentials and particle velocities. For example, the error index EI can be defined on surfaces S_1 and S_3 such that [9]

$$EI = \left\{ \int_{S_1} \left| \sum_{n=0}^N a_n \Psi_n^{(1)}(r_1, \theta) - U_v(r_1, \theta) \right|^2 dS + \int_{S_3} \left| \sum_{n=0}^N a_n \Psi_n^{(1)}(r_1, \theta) \right|^2 dS \right\} / \pi A^2 U_0^2 \quad (20)$$

The numerator is the integral of the square error of the particle velocity on surfaces S_1 and S_3 , and the denominator is the integral of the squared velocity (prescribed) on surfaces S_1 and S_3 . On surface S_2 the error index of the matching of the particle velocity is also defined in the same way as Eq. (20). (The matching of the velocity potential is always well satisfied by Eqs. (9) and (10). These indexes were less than 0.001 at the peak frequencies, except for the convex dome with $H/A = 0.7$. At both ends of the frequency range, the error indexes tend to become larger than in the midfrequency range. Using the values of M and N described at the beginning of Section 4, however, the error indexes were reasonably small in the range shown in Sections 4.1 and 4.2. From the above discussion it may be concluded that the present method has sufficient accuracy for the discussion of the radiation characteristics of the concave and convex domes in the semi-infinite tube.

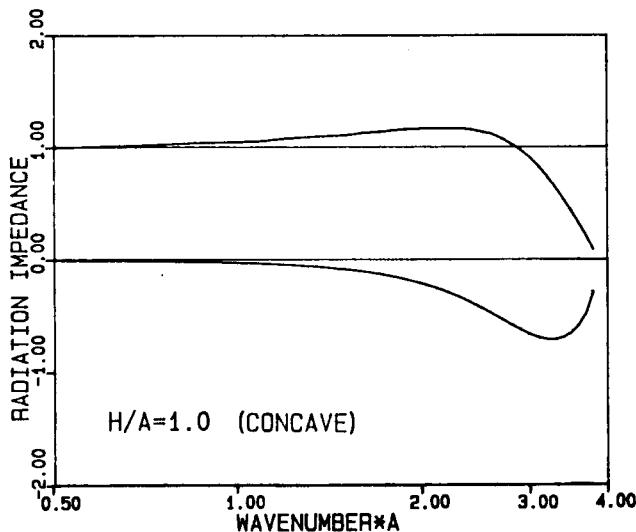


Fig. 9. Normalized radiation resistance (upper curve) and radiation reactance (lower curve) of a concave dome with $H/A = 1.0$ in a semi-infinite tube.

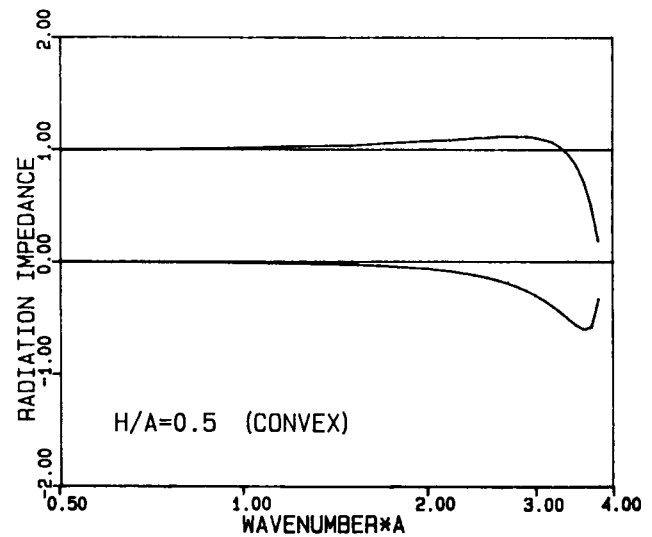


Fig. 10. Normalized radiation resistance (upper curve) and radiation reactance (lower curve) of a convex dome with $H/A = 0.5$ in a semi-infinite tube.

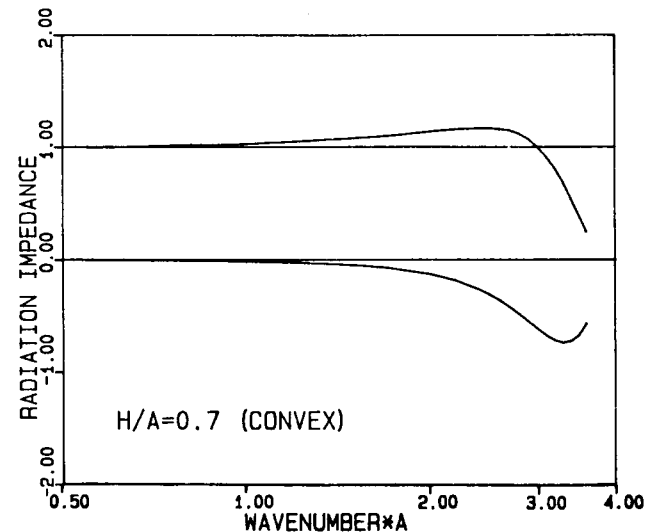


Fig. 11. Normalized radiation resistance (upper curve) and radiation reactance (lower curve) of a convex dome with $H/A = 0.7$ in a semi-infinite tube.

5 CONCLUSION

Our numerical analysis of the radiation problem of the concave and convex domes in a semi-infinite tube shows that the radiation resistance is not constant even if the diaphragm vibrates as a piston. The radiation resistance reaches its maximum value of 0.5–0.7 dB (for $H/A = 0.5$ –1.0) around the frequency range of $kA = 2.2$ –2.8. The radiation resistance then drops abruptly above this peak frequency. The radiation resistance becomes comparable with the radiation resistance above around $kA = 2.5$, but its effect on the radiation characteristics seems negligible since the mechanical impedance of the driver dominates in this range.

The deviation of the radiation resistance of the nonflat diaphragm from that of the flat piston may not be significant in most cases. It may certainly be possible, however, to experience the worst case in which the total error of the measurement system exceeds ± 2 dB (the accuracy for the measurement of sound pressure required in [11]), if we are not aware of the above-mentioned radiation characteristics of a nonflat diaphragm in a wave tube.

6 REFERENCES

[1] A Kundt, *Pogg. Ann.*, Vol. 135, pp. 337–372 (1868).

[2] J. W. S. Rayleigh, *The Theory of Sound* (Dover, New York, 1945), vol. 2, sec. 260.

[3] L. L. Beranek, "Precision Measurement of Acoustic Impedance," *J. Acoust. Soc. Am.*, vol. 12, pp. 3–13 (1940).

[4] L. Cremer and H. Millar (transl. by T. J. Schultz), *Principles and Applications of Room Acoustics* (Applied Science Publ., London and New York, 1982) vol. 2, pp. 51–69.

[5] "DRAFT AES Recommended Practice Specification of Loudspeaker Components Used in Professional Audio and Sound Reinforcement," *J. Audio Eng. Soc.*, vol. 30, pp. 141–144 (1982 Mar.).

[6] S. Ohie, R. Takeuchi, and T. Shindo, "Sound Radiation from a Concave Radiator in an Infinite Baffle," *Acustica*, vol. 46, pp. 268–275 (1980).

[7] H. Suzuki and J. Tichy, "Sound Radiation from Convex and Concave Domes in an Infinite Baffle," *J. Acoust. Soc. Am.*, vol. 69, pp. 41–49 (1981).

[8] H. Suzuki and J. Tichy, "Radiation and Diffraction Effects by Convex and Concave Domes," *J. Audio Eng. Soc.*, vol. 29, pp. 873–881 (1981 Dec.).

[9] H. Suzuki and J. Tichy, "Sound Radiation from an Axisymmetric Radiator in an Infinite Baffle," *J. Acoust. Soc. Jpn. (E)*, vol. 3, pp. 167–172 (1982).

[10] H. Suzuki and J. Tichy, "Diffraction of Sound by a Convex or Concave Dome in an Infinite Baffle," *J. Acoust. Soc. Am.*, vol. 70, pp. 1480–1487 (1981 Nov.).

[11] "IEEE Recommended Practice for Loudspeaker Measurements," IEEE Std. 219-1975.

THE AUTHOR



Hideo Suzuki studied electrical engineering at Tohoku University in Japan, where he earned B.S. and M.S. degrees. From 1967 to 1979 he worked for Mitsubishi Electric Corporation in the area of loudspeaker development and research.

Following the completion of the doctoral program in acoustics at the Pennsylvania State University in 1981, he started working for CBS Technology Center. He was engaged in the vibration and sound radiation

analysis of musical instruments, loudspeaker development, and in some other acoustics-related areas.

From 1985 September he has been at Ono Sokki in Japan, a manufacturer of measuring instruments and control systems.

He has published several papers in loudspeaker and piano acoustics in *JAES*, *JASA*, and *JASJ*. He is a member of the Audio Engineering Society and the Acoustical Society of America.